Creep Analysis of Axially Loaded Frp Concrete Columns

Hani M. Fahmi*, Ph.D.(Prof.) Ahmed Karim,** M. Sc.

Abstract

In this investigation, a three-dimensional finite element model has been used to analyze four concrete-filled fiber reinforced polymer (FRP) tubes and two fiber-wrapped concrete columns under sustained axial compressive load utilizing ANSYS software. Twenty-node viscoelastic element has been used to model the concrete, while the FRP tube is modeled using twenty-node isoparametric solid element and fiber-wrap is modeled using eight-node isoparametric shell element, both connected by eight-node isoparametric interface element. Also, the effects of some important parameters including concrete compressive strength, tube wall thickness, number of fiber-wraps, column diameter, ultimate creep coefficient, and type of FRP on the creep behavior of these columns have been investigated. Comparison between the numerical and available experimental long-term results showed good agreement with a maximum difference of the total strain values of 5.5%, which confirms the accuracy and validity of the models and materials constitutive relations and method used. The numerical results also showed that a stress transfer in the concrete-filled FRP column occurred with time between the FRP tube and the concrete, leading to a 22% stress reduction in the concrete and a stress increase in the FRP of 25% after 200 days of loading.

Keywords: Concrete, Creep, Columns, Fiber Reinforced Polymer, Finite Element Analysis, Time Effects

* Al-Mansour University College
**Al-Rafidain University College

1. Introduction

Creep is an internal characteristic of concrete under long-term load [1]. Creep analysis of fiber reinforced polymer (FRP) confined concrete is complicated due to the different creep properties of its two components. There are two types of FRP-confined concrete systems:-

a- Fiber-Wrapped Concrete Columns (FWCC), in which the wrap only provides lateral confinement to the concrete; and
b- Concrete-Filled Fiber Tubes (CFFT), in which the tube carries a proportion of the axial loads in addition to providing confinement.

The analytical issues of concern are as follows:

1- Sealing concrete from moisture migration considerably reduces its drying creep and shrinkage
2- Lateral confinement places concrete in a triaxial state of stress, which results in less creep
3- Stress transfer between the concrete and tube in CFFT leads to stress relaxation in concrete, which leads to further reduction of its creep, and
4- Stresses in each materials of the system vary with time, even though the total applied column load may remain constant.

To isolate the effects of confinement and creep of the shell from the concrete creep, steel- confined concrete may be considered as a prelude to FRP-confined concrete, simply because steel does not creep. In concrete filled steel tubes (CFST), also two types of construction are feasible:

(1) Unbonded, in which the tube only provides confinement for the concrete.
(2) Bonded, in which the tube also carries a portion of the applied loads.

Bonded tubes curtail creep of concrete much more than the equivalent unbonded tubes, mainly because of the stress relaxation phenomenon. FWCC is similar to an unbonded CFST, except that the FRP shell creeps in the hoop direction creep of the FRP tube [2].

The main objective of this research work is to carry out a numerical investigation on the time-dependent behavior of confined composite concrete columns subjected to sustained compressive loading. This aim is

achieved by using the finite element method utilizing ANSYS software, in which a three-dimensional viscoelastic finite element is used to model the concrete core, and a solid element to model the FRP tube, shell element to model the FRP-wrap and an interface element to model the contact between the concrete and the FRP.Two types of confined concrete columns CFFT and FWCC are used in the analysis, and the results obtained are compared with available experimental results Parametric studies have been carried out in order to study the effect of different factors on the behavior of CFFT and FWCC columns under long-term loading including concrete compressive strength, fiber tube wall thickness, number of fiber wrap layers, column diameter, and ultimate creep coefficients on the overall behavior of FRP confined concrete columns .

2. Finite Element Analysis

2.1 Viscoelasticity In ANSYS Program

A material is said to be viscoelastic if it has an elastic (recoverable) part as well as a viscous (non-recoverable) part. Upon application of the load, the elastic deformation is instantaneous, while the viscous part occurs over time. Generally, the stress function of a viscoelastic material is given in an integral form. Within the context of small strain theory, the constitutive equation for an isotropic viscoelastic material can be written as:

$$\sigma = \int_0^t 2G(t-\tau)\frac{de}{d\tau}d\tau + \mathrm{I}\int_0^t \mathrm{K}(t-\tau)\frac{d\Delta}{d\tau}d\tau \qquad \text{... (1)}$$

where:

σ **=** Cauchy stress.
e = deviatoric part of strain.
Δ = volumetric part of strain.
$G(t)$ = shear relaxation kernel function.
$K(t)$ = bulk relaxation kernel function.
t = current time.
τ **=** elapsed time at loading, and

I = unit tensor.

For the viscoelastic element in ANSYS (VISCO89), the material properties are expressed in integral form using the kernel function of generalized Maxwell elements as:

$$G(\xi) = G_\infty + \sum_{i=1}^{n_G} G_i e^{\left(-\xi / \lambda_i^G\right)} \quad \text{... (2)}$$

$$\mathrm{K}(\xi) = \mathrm{K}_\infty + \sum_{i=1}^{n_\mathrm{K}} \mathrm{K}_i e\left(-\xi / \lambda_i^\mathrm{K}\right) \quad \text{... (3)}$$

$$G_i = C_i\left(G_0 - G_\infty\right) \quad \text{... (4)}$$

and

$$\mathrm{K}_i = D_i\left(\mathrm{K}_0 - \mathrm{K}_\infty\right) \quad \text{... (5)}$$

where:

ξ **=** reduced or pseudo time = t-t'.

i = number of Maxwell elements used to approximate the material's relaxation shear modulus.

$G(\xi)$ = shear relaxation kernel function.

$\mathrm{K}(\xi)$ = bulk relaxation kernel function.

n_G = number of Maxwell elements used to approximate the shear relaxation kernel.

n_K **=** number of Maxwell elements used to approximate the bulk relaxation kernel**.**

C_i **=** constants associated with the instantaneous response for shear behavior.

D_i **=** constants associated with the instantaneous response for bulk behavior.

G_0 **=** initial shear modulus.

G_∞ **=** final shear modulus.

K_0 **=** initial bulk modulus**.**

K_∞ **=** final bulk modulus.

λ_i^G **=** constants associated with a discrete relaxation spectrum in shear.

λ_i^K **=** constants associated with a discrete relaxation spectrum in bulk.

2.2 Material Representation for ANSYS Solution

From the previous section, it is clear that ANSYS program will need material characteristics such as initial and final shear moduli, number of Maxwell elements with relaxation modulus and discrete relaxation spectrum for each Maxwell element assuming constant temperature and stress behavior along the age of the structure indicated by the bulk modulus. Obtained by fitting the compliance function from ACI Committee 209R Eqs. (6), (7) and (8) using a specially written program of least squares method for curve fitting to a polynomial. Prony Series Fitting Program (PSFP) coded in Visual Fortran 5.0 language is used for obtaining Prony series representation of reduction of shear modulus.

$$\left.\begin{aligned} \gamma_{la}^{c} &= 1.25\tau^{-0.118} \quad \textit{for moist curing} \\ &= 1.13\tau^{-0.094} \quad \textit{for steam curing} \end{aligned}\right\} \quad ...(6)$$

$$G = \frac{E}{2(1+\upsilon)} \quad \textbf{... (7)}$$

$$\mathrm{K} = \frac{\mathrm{E}}{3(1-2\upsilon)} \quad \textbf{... (8)}$$

K **=** bulk modulus.

In the first which one enters the load duration of each case, and finds the reduction of Young's modulus of concrete at each time using Eq. (6), then finds the shear modulus at each load using Eq. (7) (according to ACI Committee), then enters the load duration and shear modulus as a matrix in the Fortran program. Then final shear modulus and the constants associated with the instantaneous response for shear behavior (C_i) are obtained. After obtaining agreement of the results of this program with the results obtained by Eq.

$$\Delta\varepsilon = \frac{\Delta\sigma}{\mathrm{E}(\mathrm{t_o})} + \frac{1}{2}[\sigma(\mathrm{t_o}) + \sigma(\mathrm{t})]\frac{\varphi(\mathrm{t},\mathrm{t_o})}{\mathrm{E}(\mathrm{t_o})}$$

the programs results of this program are input into ANSYS program to get the bulk modulus according to Eq. (8).

3. Finite Element Formulation

3.1 Concrete Core and FRP-Tube Idealization

The concrete core and FRP-tube are modeled using 20-node quadratic isoparametric brick element (VISCO89 and SOLID95 in ANSYS 10), as shown in Fig.1. The element is defined by 20nodes having three degrees of freedom at each node: u, v and w in the X, Y and Z directions, respectively. The element has thermorheologically simple viscoelastic and stress stiffening capabilities

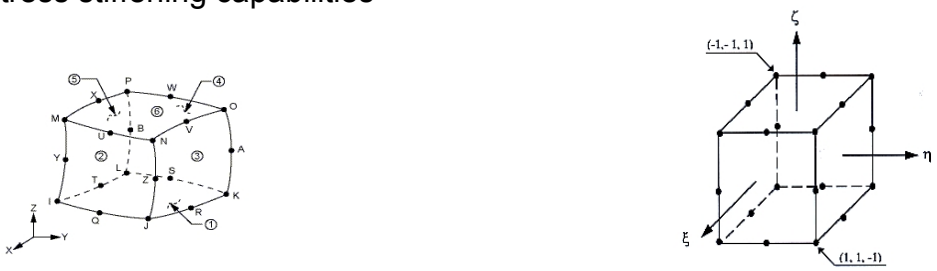

a. Cartesian coordinate system **b.** Natural coordinate system

Figure 1 VISCO89 and SOLID95 Viscoelastic Solid Elements [6]

3.2 FRP Sheet Idealization

The 8-node isoparametric shell element (SHELL93) is used to model the FRP sheet in the composite column, in which the deformation shape functions are quadratic in both in-plane directions, as shown in Fig. 2.The element has six degrees of freedom at each node: three translations in the nodal x, y and z directions and three rotations about the x, y and z-axes. The element also has plasticity, stress stiffening, large deflection, and large strain capabilities.

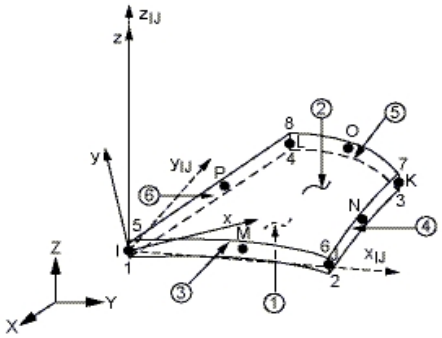

Figure 2 Eight-node isoparametric shell element [6].

3.3 Interface Model

To model the interface behavior between the concrete and fiber, the 8-node surface contact element (CONTA174) shown in Fig. 3, has been used. The element models contact and sliding between 3-dimensional target surface and a deformable surface defined by this element. The element is applicable to 3-D structural and coupled field contact analyses. This element is used on the surfaces of 3-D solid or shell elements with midside nodes; it has the same geometric characteristics as the solid or shell element face with which it is connected. This element has three degree of freedom at each node u, v and w.The element is intended for general rigid-flexible and flexible-flexible contact analysis. Contact occurs when the element surface penetrates one of the target segment elements, a specified target surface. Both Coulomb and shear stress friction are allowed.

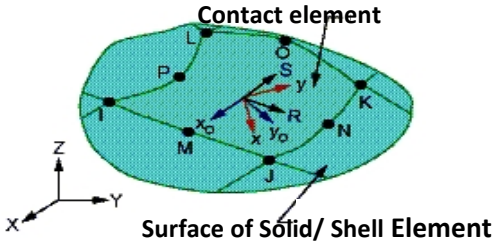

Figure 3 Eight-node surface contact element [6].

4. Numerical Integration

Generally, it is impossible to perform analytically the integrations necessary to set up the stiffness matrices of isoparametric element. Therefore, resort has to be made to some suitable scheme of numerical integration. In finite-element work, one particular scheme which has been found to be very useful, is Gauss (or Gauss-Legendre) numerical integration. For a given accuracy, Gauss method requires the least number of points of the function being integrated. In two-dimensional problems, determining the stiffness matrix of an isoparametric quadrilateral element requires evaluating definite integral of the form is

$$\mathrm{I} = \int_{-1}^{+1}\int_{-1}^{+1} F\left(\xi,\eta\right)\, d\xi d\eta$$

i.e., the integral of function F with respect to ξ and η in the range –1 to +1.

The idea just described can be readily extended to three-dimensional cases, in which the properties of an isoparametric brick element are to be evaluated, i.e. integrals of the following arise:

$$I = \int_{-1}^{+1}\int_{-1}^{+1}\int_{-1}^{+1} F\left(\xi\left(\eta,\zeta\right)\right) d\xi d\eta d\zeta \qquad \text{... (9)}$$

and can be evaluated numerically as:

$$I = \sum_{i=1}^{ni}\sum_{j=1}^{nj}\sum_{k=1}^{nk} W_i W_j W_k F\left(\xi_k,\eta_j,\zeta_i\right) \qquad \text{... (10)}$$

The question arises as to what level of numerical integration should be used in evaluating the element properties. It is known that in one-dimensional analysis, the use of n integration points in the Gaussian Quadrature procedure provides exact evaluation of the integral of any polynomial of degree $2n-1$ or less. In two and three-dimensional analyses, this rule applies in each coordinate direction in Fig.4. numerical integration using the indicated points would be exact for a polynomial of up to third order in each of the ξ and η directions. Now, although it might appear at first that the integration procedure should be carried out exactly

or at least as close to the exact as possible, this in fact is rarely the aim. The position of Gauss points for $n = 2$ that is for 2×2×2 integration rule for shell and interface elements, while the twenty seven (3x3x3) Gaussian rule exactly integrates the stiffness matrix of twenty-node quadratic viscosolid element, as shown in Fig.4. A list of sampling points and weighting factors are given in Table 1

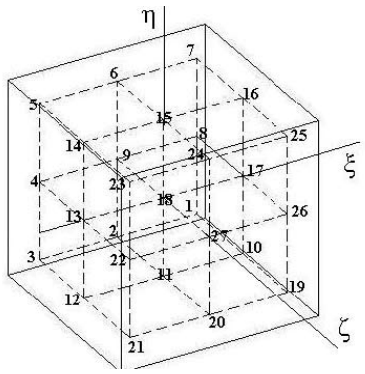

Fig.4 Distribution of sampling points
for 3-dimensional element in 27 Gaussian points integration rule

Table 1 Weights and abscissa of sampling point's integration rule.

Integration rule	Sampling Point number	Local coordinates			Weight
		ξ	η	ζ	
2x2	1 to 4		$\mp 1/\sqrt{3}$	$\mp 1/\sqrt{3}$	1
3x3x3	1,3,5,7,19,21,23,25	$\pm$ 0.7746	$\pm$ 0.7746	$\pm$ 0.7746	0.17146
	2,6,20,24	0	$\pm$ 0.7746	$\pm$ 0.7746	0.27434
	4,8,22,26	$\pm$ 0.7746	0	$\pm$ 0.7746	0.27434
	10,12,14,16	$\pm$ 0.7746	$\pm$ 0.7746	0	0.27434
	13,17	$\pm$ 0.7746	0	0	0.43895
	9,27	0	0	$\pm$ 0.7746	0.43895
	11,15	0	$\pm$ 0.7746	0	0.43895
	18	0	0	0	0.70233

5. ANSYS Computer Program

As mentioned before, the finite element analysis has been carried out utilizing ANSYS computer program [5]. It is used to analyze CFFT & FWCC columns. This program has the capacity of solving linear and nonlinear problems, static, dynamic, thermal, and conductivity, problems
This program has a comprehensive graphical user interface (GUI) capability that gives users easy, interactive access to program functions, commands, documentation, and reference material. An intuitive menu system helps users to navigate through the ANSYS program. Users can input data using a mouse, a keyboard, or a combination of both.

6. Numerical Analysis

Table 2 Properties of the concrete used in the analysis of the FRP columns [5]

Properties	Columns				
	C1	C2	C3	C4	F1and F2
Compressive strength f'_c, MPa	38	38	38	38	29
Concrete modulus of elasticity *E_c, MPa	28972.75	28972.75	28972.75	28972.75	25310.28
Initial shear modulus G_0, MPa	12600.34	12600.34	12600.34	12599.43	11007.65
Final shear modulus G_∞, MPa	8406.88	8077.45	8070.11	7972.29	6788.66
Bulk modulus k, MPa	13796.55	13796.55	13796.55	13796.55	12052.5
Poisson's ratio υ_c	0.15**	0.15**	0.15**	0.15**	0.2**
Age at loading t_{la}, days	556	64	276	53	21
Relative humidity H, %	100**	100**	100**	100**	100**
Slump S, mm	76	76	76	76	76
Cement content c_m, kg/m^3	400	400	400	400	350
Fine aggregate ratio,%	60**	60**	60**	60**	60**
Air content , %	4**	4**	4**	4**	4**

* $\mathrm{E}_c = 4700\sqrt{f'_c}$.

** assumed

7. Analysis of Concrete-Filled FRP Tube Columns

The concrete filled FRP tube C1, C2, C3 and C4, in which the tubes were made from E-glass fibers, have 152mm outside diameter and 16mm tube thickness of, and 915mm length. The columns consist of a resin-rich inner layer, and mid layer between the two centrifuge batches [5]. The compressive loads are applied at the top of the columns as a pressure and kept constant through the analysis. The applied loads are 56, 194.4, 142 and 120 kN for columns C1, C2, C3 and C4, respectively. The properties of the E-glass fiber tube of the CFFT columns used in the analysis are:

E_f = 23257 MPa, and assumed v_f = 0.15

7.1 Finite Element Idealization and Material Properties

Columns C1, C2, C3 and C4, are analyzed by the finite element method utilizing the computer program ANSYS 10. The columns are modeled by 717 20-node viscoelastic solid elements (VISCO89) for the concrete core and by 1037 20 -node isoparametric solid elements (SOLID95)for fiber tube connected by 208 8-node isoparametric interface elements (CONTA174), i.e. a total of 1962 elements are used. The finite element analysis has been carried out using 27-point (3×3×3) integration rule for the concrete viscoelastic solid elements and for both the FRP-tube solid elements, and 4-point (2×2) integration rule for the interface elements. Details of the finite element mesh, boundary conditions and loading used are shown in Figs. 5 and 6.

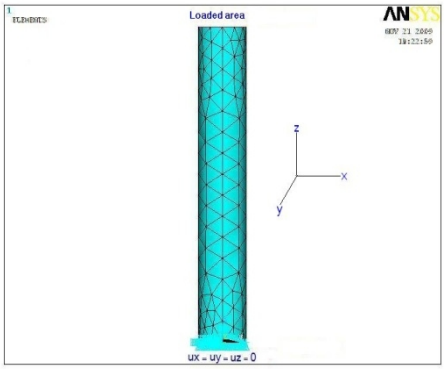

Fig. 5 Model and boundary conditions for CFFT Columns.

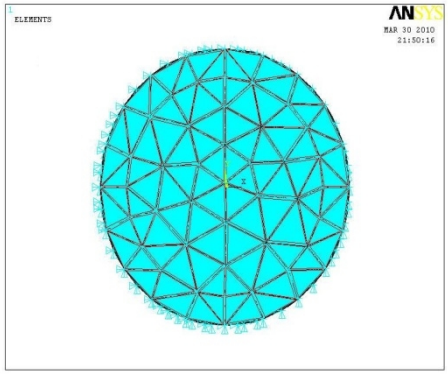

Fig. 6 Top view of the model for CFFT Columns.

7. 2 Results of Analysis and discussions

The numerical and experimental total strain (elastic creep) time curves obtained for the CFFT columns C1, C2, C3 and C4, are shown in Figs.(7), (8), (9) and (10), respectively. The figures show that the finite element results are in good agreement with the experimental results throughout the entire range of loading and that the numerical total strains after 160 days loading for columns C1,C2 and C4 and 200 days for column C3 are 564×10^{-6}, 4440×10^{-6}, 2545.5×10^{-6} and 2027×10^{-6} for columns C1, C2, C3 and C4, respectively while the experimental total strain values were 560×10^{-6}, 4417×10^{-6}, 2543×10^{-6} and 2026×10^{-6}, respectively. The differences between the numerical and experimental total strain values are 4.76%, 5.23%, 5.5% and 3.7%, respectively. It can be noticed from Fig. (6) that a small total strain took place with time in column C1, because its applied load and ultimate creep coefficient used were less than those for the other three columns. Fig. (8) for column C2 shows that larger axial strain took the place with time, because its applied load and ultimate creep coefficient were larger than those for other columns. In fact, when total strains exceed the range of (0.002-0.003), creep effects need to be considered [5], these cases can be seen in Figs. (8), (9) and (10), for columns C2, C3 and C4, respectively. Figures (11) and (12) show that specific total strains decrease with the increase of concrete age at loading. The specific total strain values are 2027×10^{-6}, 2440×10^{-6}, 2542.5×10^{-6} and 564×10^{-6} when the ages at loading used are 53, 64, 276and 556 days for the CFFT columns C4, C2, C3and C1, respectively.

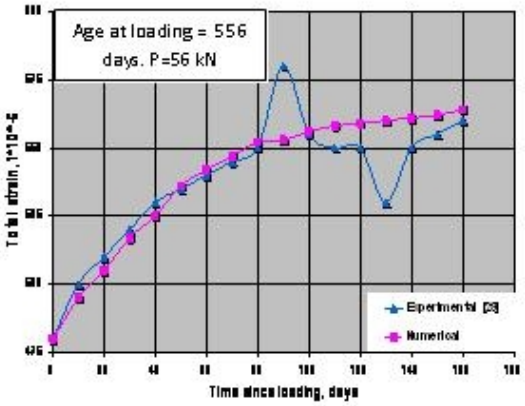

Fig. 7 Numerical and experimental total strain-time relation for CFFT Column C1.

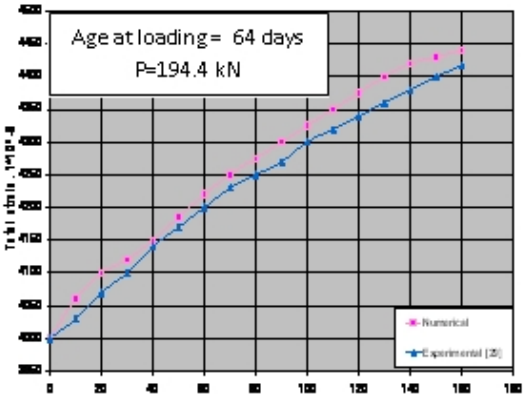

Fig. 8 Numerical and experimental total strain-time relation for CFFT Column C2.

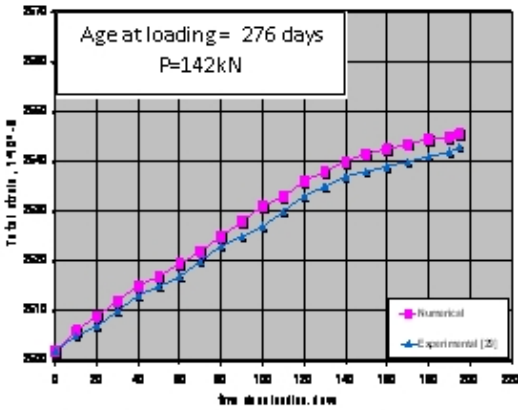

Fig. 9 Numerical and experimental tota strain-time relation for CFFT Column C

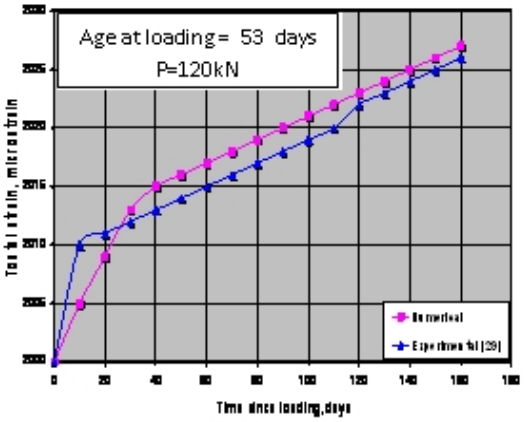

Fig. 10 Numerical and experimental total strain-time relation for CFFT Column C4.

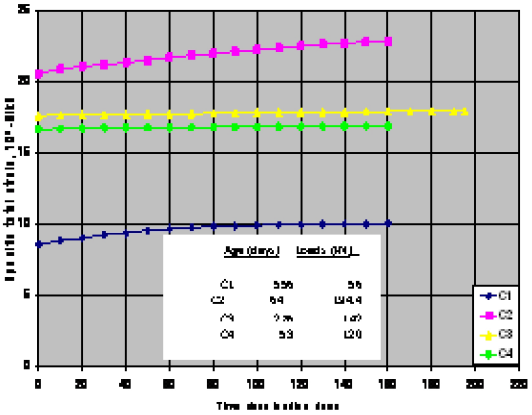

Fig. 11 Numerical specific total strain-time relation for CFFT Columns C1, C2, C3 and C4.

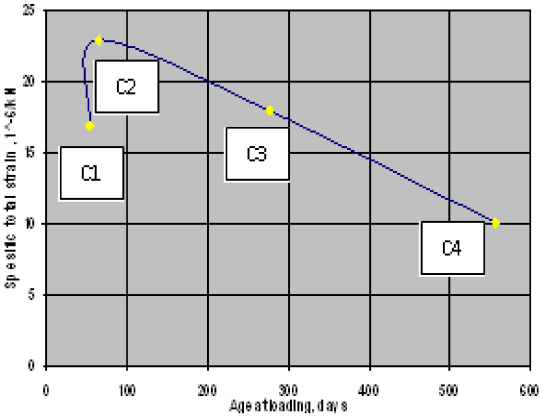

Fig. 12 Numerical specific total strain-age at loading relation of CFFT Columns C1, C2, C3 and C4 after 160 days of loading.

The axial stress transfer between the concrete and the FRP tube in CFFT columns leads to stress reduction in the concrete, thus further reducing its creep, and stresses in each component of the system vary with time, even though the total applied load remains constant. Figures (13) to(16) show that axial stress redistribution takes place in CFFT concrete columns between the concrete the FRP tube based on the model prediction. Axial stresses in the FRP tubes increase by 31%, 23%, 25% and 24%, while 20%, 19.5%, 22% and 19% stress reductions occur in the concrete for columns C1, C2, C3 and C4, respectively. Figure (16) shows the stresses in the FRP tube of column C4 after 160 days of loading.

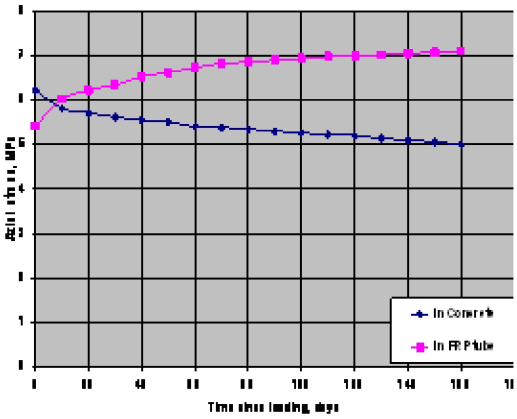

Fig. 13 Numerical axial stress-time relation for concrete core and FRP tube in CFFT Column C1.

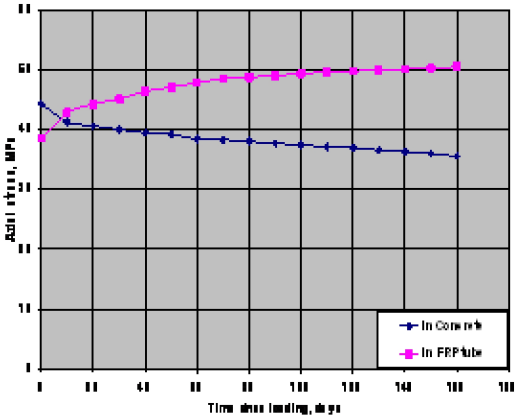

Fig. 14 Numerical axial stress-time relation for concrete core and FRP tube in CFFT Column C2.

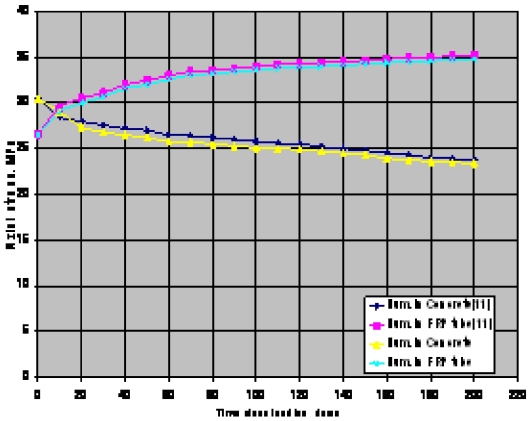

Fig. 15 Numerical axial stress-time relation for concrete core and FRP tube in CFFT Column C3.

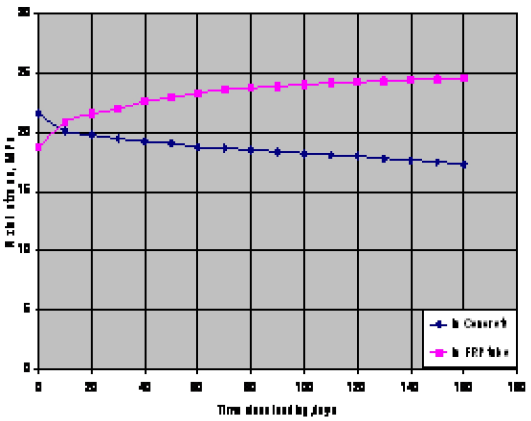

Fig. 16 Numerical axial stress-time relation for concrete core and FRP tube in CFFT Column

8. Analysis of Fiber-Wrapped Concrete Columns

Two fiber-wrapped concrete columns F1 and F2 (FWCC) are analyzed. The wrap these columns is made with two 1 mm thick layers of uniaxial E-glass fibers with epoxy resin at a fiber volume fraction of 35.4% [5]. The columns outside diameter of 152mm and 915mm length. The compressive load is applied at the top of the column as a pressure and kept constant

through the analysis. Loads of 39 and 76.7 kN are applied at the top of columns F1 and F2, respectively. The properties of the FRP wrap of the FWCC columns used in the analysis are:

E_f = 26135 MPa, and assumed v_f = 0.15

8.1 Finite Element Idealization and Material Properties

The fiber-wrapped concrete columns F1 and F2, are analyzed by the finite element method utilizing the computer program ANSYS. The columns are modeled by 2950 20-node viscoelastic solid elements (VISCO89) for the concrete core and by 373 8-node isoparametric shell elements (SHELL93), both connected by 373 8-node isoparametric interface elements (CONTA174), i.e.a total of 3696 elements are used. The finite element analysis has been carried out, using 27-point (3×3×3) integration rule for the concrete viscoelastic solid elements, and 4-point (2×2) integration rule for the FRP laminate shell and the interface elements.

8.2 Results of Analysis and Discussion for Fiber Wrapped Concrete Columns

The numerical and experimental total strain (elastic creep) time curves for columns F1and F2, are shown in Figs. (17) and (18), respectively. These figures show good agreement between the numerical and experimental results throughout the entire range of loading. It can be seen from the figures that the computed total strains after a period of 100 days are 557×10^{-6} and 1240×10^{-6}, while the experimental values were 550×10^{-6} and $1263\times10^{-6,}$ for columns F1 and F2, respectively.The maximum difference between numerical and experimental total strain values is 5.52% and 4.97%, respectively. Since the FRP wraps in FWCCs cannot carry any axial load, there is no redistribution of axial stresses between the wrap and concrete core. The wrap in this case only provides confinement [5]. Fig. (19) shows that specific total strains decrease with the increase of applied load for the same age at loading.

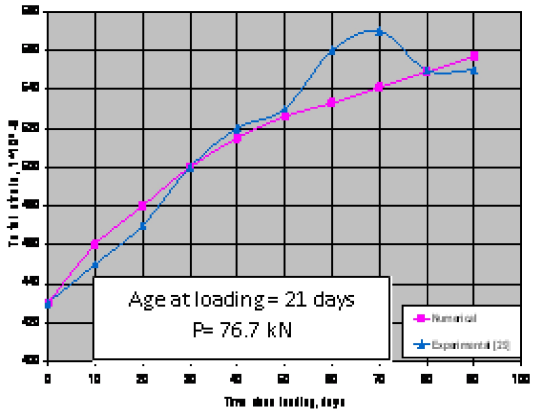

Fig. 17 Numerical and experimental total strain-time relations for FWCC Column F1.

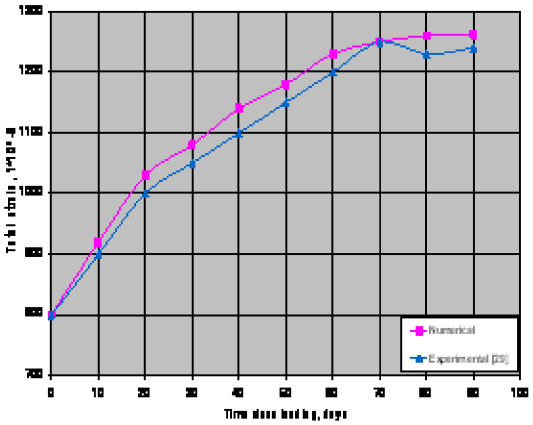

Fig. 18 Specific total strain-time relation for FWCC Columns F1 and F2.

The axial stress transfer between concrete and th FRP wrap in FWCC columns leads to stress reduction in the concrete, further reducing its creep, and stresses in each component of the system may vary over time, even though the total applied load may remain constant. Figures(20) and (21), show that axial stress redistribution takes place in FWCC concrete columns , the axial stresses in the FRP tube increases by 21% and 22%, while 13.5% and 15% stress reductions occur in concrete core for columns F1 and F2, respectively. Table 3 shows a summary of the computed FRP column results.

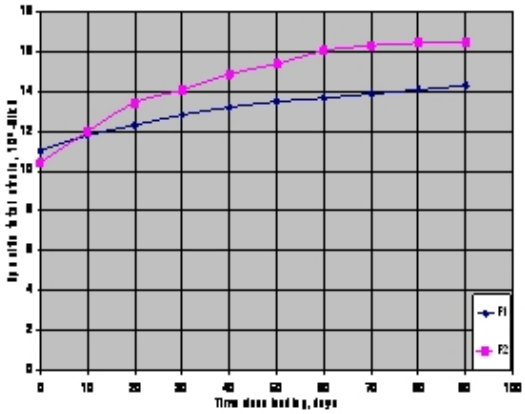

Fig. 19 Numerical specific total strain-time relation for FWCC Columns F1 and F2.

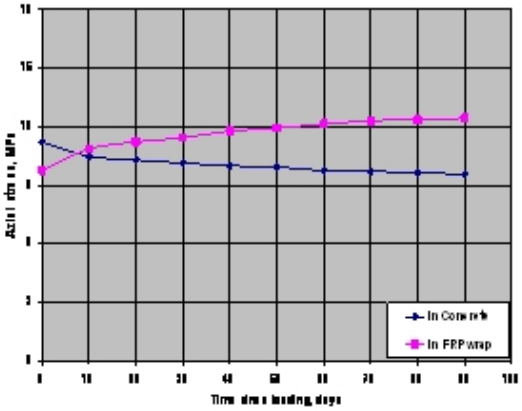

Fig. 20 Numerical axial stress-time relation for concrete core and FRP wrap in FWCC Column F1.

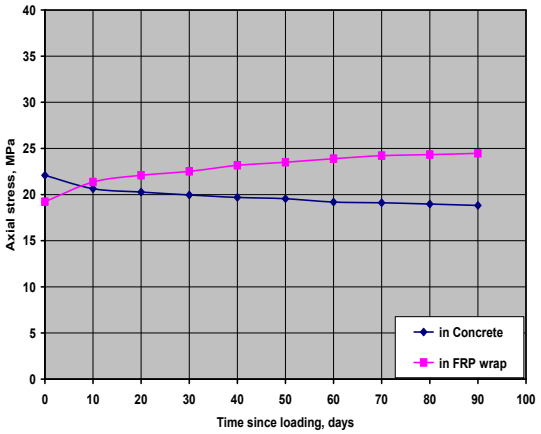

Fig. 21 Numerical axial stress-time relation for concrete core and FRP wrap in FWCC Column F2.

Table 3 Summary of the computed FRP concrete Columns results.

Variables	Columns					
	C1	C2	C3	C4	F1	F2
Applied load, (kN) (1)	56	194.4	142	120	39	76.7
Age at loading, (days) (2)	556	64	276	53	21	21
Loading period, (days) (3)	160	160	200	160	90	90
Exp. total strain, (1×10^{-6}) (4)	560	4417	2543	2026	550	1240
Num. total strain, (1×10^{-6}) (5)	564	4440	2545	2027	557	1263
Ultimate load, (kN) (6)	585	585	585	585	237.5	237.5
Total strain ratio (7)=(5)/(4)	1.007	1.005	1.001	1.000	1.013	1.019
Applied load ratio, % (8)=(1)/(6)	9.5	33	24	21	16	32
Num. specific total strain, (1×10^{-6}) (9)=(5)/(1)	10.07	22.84	17.93	16.89	14.82	16.47

9. Parametric Study

In order to investigate the effect of some of the main parameters that may influence the time- dependent behavior of FRP columns, a parametric study is carried out on the columns with one parameter being changed at a time, while the others are kept constant, in order to find the effects of the parameter considered.

9.1 Effect of Concrete Compressive Strength

Analysis for the time- dependent effect of concrete compressive strength f'_c is carried out on CFFT column C1, which had a compressive strength of 38 MPa. Compressive strength values of 28, 50 and 60 MPa are considered in the analysis.

It can be observed from Fig.22 that the long-term total strain of the composite column decreases with the increase of concrete compressive strength. The total strain increased by 2.5 % for a decreased concrete compressive strength of 28 MPa while increasing the strength to 50 and 60 MPa results in a 2.8 and 3.3 % decrease in the total strain of the column, respectively.

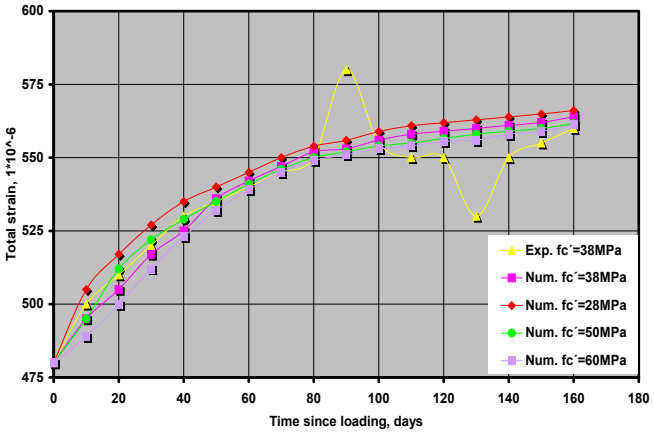

Fig. 22 Effect of concrete compressive strength on the total strain of CFFT Column C1.

9.2 Effect of Fiber Tube Wall Thickness

The effect of Fiber tube wall thickness is carried out through the analysis of CFFT column C3, which has a thickness of 1.6 mm. Fig. (23) shows the effect of wall thickness on the of total strain-time curves for column C3. The long-term total strain is increased by 35 % when the tube wall thickness is reduced from 16 to 10 mm, while increasing the wall thickness to 20 mm results in a 13% reduction in the long-term strain after 200 days of loadings.

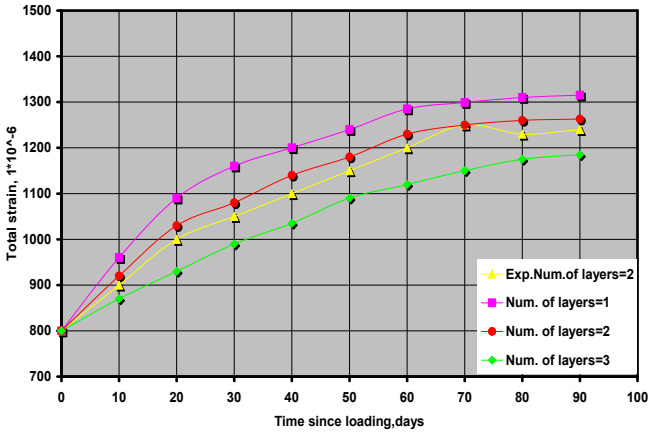

Fig. 23 Effect of fiber tube wall thickness on the confined behavior of CFFT Column C3.

9.3 Effect of Number of Fiber Wrap Layers

In order to study the effect of the number of fiber wrap layers as FWCC column F2, which had two layers and a difference of one layer are considered in the analysis. Fig. (24) shows that the total-strain increases with the decrease of the number of fiber wrap layers. The figure also shows that an increase from two to three of layers caused a decrease of about 13% in the total strain of the FWCC column, while a decrease in the number of layers from two to one caused an increase of about 11 % in the total strain after 200 days of loading.

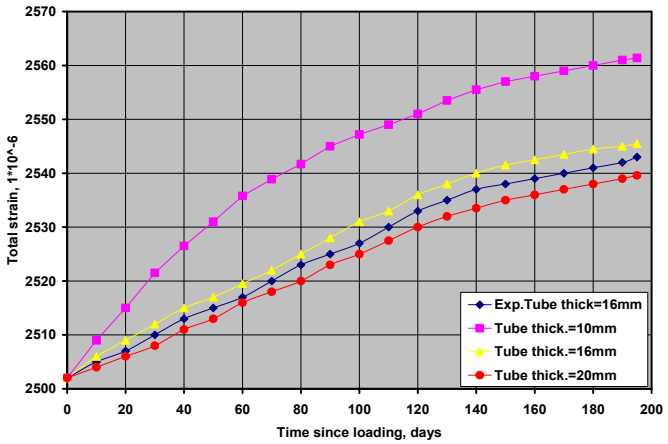

Fig. 24 Effect of fiber wrap layers on the behavior of FWCC Column F2.

9.4 Column Diameter

Columns C2 which had a diameter of 152 mm has been analyzed to study the effect of column diameter on the long-term strain of FRP concrete columns. Different values of the column diameters of 114, 152, 190 and 228 are considered and the results are shown in Fig. (25). The figure shows that in general the total strain decreases with the increase of column diameter. That an increase in the column diameter to 190 and 228mm under the same sustained load caused after 160 days of loading a decrease in the total strain of 27 and 53 %, respectively. While reducing the diameter to 122mm results in an increase of about 28 % in the total strain value.

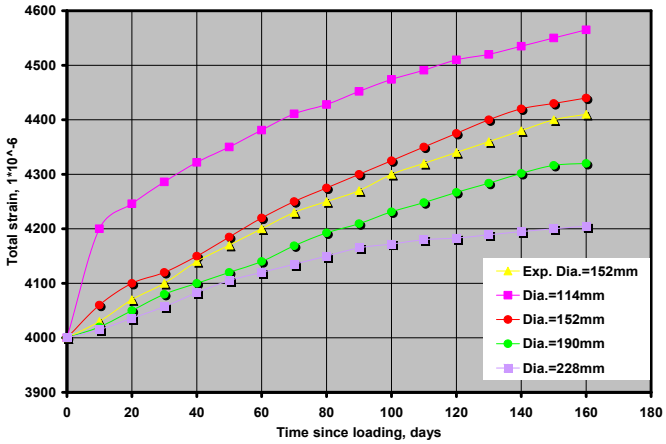

Fig. 25 Effect of outside Column diameter on the long-term behavior of CFFT Column C2.

9.5 Effect of Ultimate Creep Coefficient

The effect of creep level is considered by using different ultimate creep coefficients in the long term strain analysis carried out column C4, which had a value of 1.175. Fig. (26) shows that the total-strain of CFFT column increases as the ultimate creep coefficient is increased. The figure also shows that an increase in the ultimate creep coefficient of about 15 and 35 % caused an increase of about 2.6 and 7 % in the total strain values, while a decrease in the coefficient of 15 % caused a decrease of about 2.8 % in the total strain value after a loadings period of 160 days.

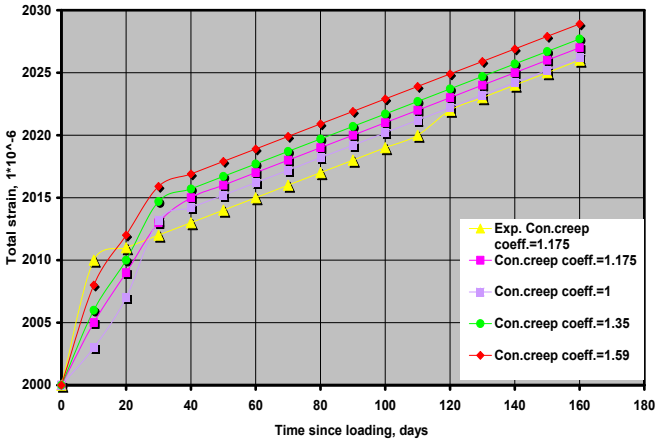

Fig. 26 Effect of concrete creep level on the long-term behavior CFFT Column C4.

9.6 Effect of Type of FRP

In order to study the affect of type of FRP on the total strain of FRP concrete columns, column C2 is chosen for the analysis. Fig. (27) shows the total strains for the unconfined, confined by GFRP, and confined by CFRP columns. The figure shows that the total strain after 160 days of loading for carbon fiber polymer (CFRP) columns is decreased by 31% in comparison with that confined by GFRP, whereas the total strain is increased by 43% for the unconfined column.

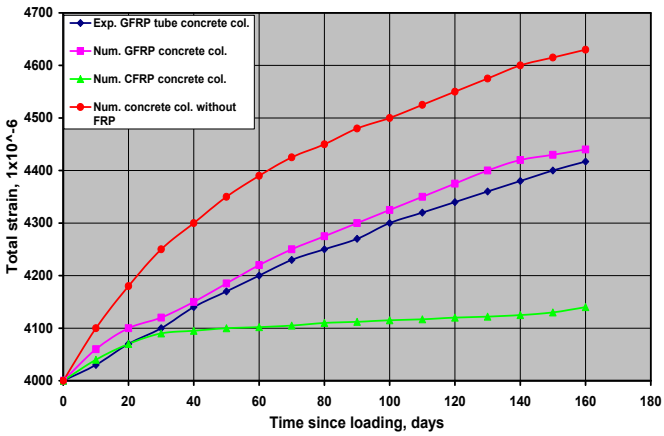

Fig. 27 Effect of FRP type on the long-term behavior CFFT Column C2.

10. Conclusions

Based on the results of the finite element analysis carried out for the concrete-filled FRP tube and fiber-wrapped concrete columns subjected to sustained loading in this investigation, the following conclusions are made:

1. Comparison of the numerical results with available experimental results, verified that the finite element models and constitutive relations and procedure used utilizing ANSYS computer program are capable and accurate to predict the time-dependent behavior of concrete-filled FRP tube columns and fiber-wrapped concrete columns.
2. Concrete compressive strength affects the total (elastic creep) strain of CFFT columns. An increase of $fc^{/}$ from 38 to 50 and 60 MPa results in 2.8 and 3.3% decrease in the total strain after 160 days of loading. On the other hand, a reduction in $fc^{/}$ to 28 MPa caused an increase of about 2.5 % in the total strain value.
3. The long-term total strain of concrete-filled FRP tube columns decrease with the increase of fiber tube wall thickness, it increased by 35% when the tube wall thickness is reduced from 16 to 10mm , while increasing the wall thickness to 20mm results in a 13% reduction in the total strain value.
4. The long-term strains of fiber-wrapped concrete columns decrease with the increase of the number of fiber wrap layers, an increase in the number of layers from two to three caused a decrease of about 13 % in the total strain, while a decrease from two to one in the number of layers caused an increase of about 11%.
5. The FRP column diameter affects on the total time-dependent strain of the columns, the total strain increase with the decrease of the column diameter, an increase in the column diameter to from 152 to 190 and 288mm caused a decrease of 27 and 53% in the long-term strain respectively, whereas a decrease of the diameter to 122mm causes an increase of 28 % in the long-term strain.
6. The concrete creep characteristics has an important effect on the long-term strains of concrete-filled FRP tube columns, an increase in its value after loadings period of 160 days of about 15 and 35 % caused an increase in the total time-dependent strain of 2.6 and 7 %

respectively, whereas a decrease of 15% caused a decrease in the total strain of 2.8%.

7. The type of FRP confinement used affects the total strain of CFFT columns. For the CFRP confinement the total strain is decrease by 31% in comparison with that confined by GFRP, whereas the total strain is increased by 43% for the unconfined column.

References

1. Cheng, X., Li, G., and Ye, G., **"Three-Dimensional Nonlinear Analysis of Creep in Concrete-Filled Steel Tube Columns",** Journal of Zhejiang University Science, Vol. 6A, No. 8, 2005, pp. 826-835.
2. Naguib, W., and Mirmiran, A**., "Creep analysis of Axially Loaded Fiber Reinforced Polymer-Confined Concrete Columns", Journal of Engineering Mechanics,** ASCE, Vol. 129, No. 11, November 1, 2003, pp. 1308-1319.
3. Hameed, Y. M., **"Nonlinear Finite Element Analysis of Reinforced Concrete Beams Strengthened with Fiber Reinforced Polymer",** M.Sc. Thesis, University of Al-Mustansiriya, 2006, 118 p.
4. ACI Committee 440 (1996**), " State of the Art Report on Fiber Reinforcement for Concrete Structures",** American Concrete Institute , Farmington Hills , Michigan, Februrary 1996,PP.68, as cited in Ref. [3].
5. Naguib, W., and Mirmiran, A.,**"Time-Dependent Behavior of FRP-Confined Concrete Columns",** ACI Structural Journal, Vol. 99, No. 2, March-April, 2002, pp. 142-148.
6. **ANSYS Manual, version 10.0, 2005.**

تحليل الاعمدة الخرسانية المحصورة بالياف البوليمر المسلحة والمحملة محوريا

أ.د. هاني محمد فهمي* أحمد كريم** (ماجستير)

المستخلص

تم في هذا البحث استخدام عناصر محددة ثلاثية الأبعاد لتحليل اربعة أنابيبب ألياف البوليمر المملؤة بالخرسانة وعمودين من الخرسانة الملفوفة بألياف البوليمر تحت حمل انضغاط محوري مستمر باستخدام برنامج الحاسوب (ANSYS). تم استخدام عنصر لزج-مرن ذو عشرين عقدة لتمثيل الخرسانة، و عنصر صلب ذو عشرين عقدة لتمثيل أنبوب ألياف البوليمر المسلح ، وعنصر قشري ذو ثمان عقد لتمثيل ألياف اللف, وتم ربط العنصرين باستخدام عنصر بيني ذو ثمان عقد. تم ايضا دراسة تأثير بعض المتغيرات المهمة كمقاومة انضغاط الخرسانة، سمك جدار الأنبوب، قطر العمود الخرساني، وعدد لفات الليف، مستوى الزحف النهائي, و نوع الباف البوليمر المسلحة على سلوك هذه الأعمدة. اظهرت النتائج العددية طويلة الامد لكافة الاعمدة توافقا جيدا بالمقارنة مع النتائج المختبرية المتوفرة وكان أعلى اختلاف في الانفعال الكلي بين النتيجتين حوالي 5.5% مما يؤكد دقة وصلاحية النماذج والعلاقات التكوينية للمواد والطريقة المستخدمة في التحليل.أظهرت النتائج العددية أيضا حصول انتقال في الاجهاد المحوري في عمود انبوب البوليمر المسلح بين الخرسانة وأنبوب البوليمر مع فترة التحميل, حيث انخفض الإجهاد المحوري في الخرسانة بمقدار 22% وازداد في في الاسطوانة البوليمرية بمقدار25% بعد 200 يوم من التحميل.

الكلمات المفتاحية: الخرسانة، الزحف، الاعمدة، الياف البوليمر المسلحة، التحليل بطريقة العناصر المحددة، تاثيرات الزمن

* كلية المنصور الجامعة
** كلية الرافدين الجامعة